Role of the DNA Methyltransferase Variant DNMT3b3 in DNA Methylation

Daniel J. Weisenberger, Mihaela Velicescu, Jonathan C. Cheng, Felicidad A. Gonzales, Gangning Liang, and Peter A. Jones

Urologic Cancer Research Laboratory, Department of Biochemistry and Molecular Biology, University of Southern California/Norris Comprehensive Cancer Center, Keck School of Medicine, Los Angeles, CA

Abstract

Several alternatively spliced variants of DNA methyltransferase (DNMT) 3b have been described. Here, we identified new murine Dnmt3b mRNA isoforms and found that mouse embryonic stem (ES) cells expressed only Dnmt3b transcripts that contained exons 10 and 11, whereas the Dnmt3b transcripts in somatic cells lacked these exons, suggesting that this region is important for embryonic development. DNMT3b2 and 3b3 were the major isoforms expressed in human cell lines and the mRNA levels of these isoforms closely correlated with their protein levels. Although DNMT3b3 may be catalytically inactive, it still may be biologically important because *D4Z4* and satellites 2 and 3 repeat sequences, all known DNMT3b target sequences, were methylated in cells that predominantly expressed DNMT3b3. Treatment of cells with the mechanism-based inhibitor 5-aza-2′-deoxycytidine (5-Aza-CdR) caused a complete depletion of DNMT1, 3a, 3b1, and 3b2 proteins. Human DNMT3b3 and the murine Dnmt3b3-like isoform, Dnmt3b6, were also depleted although less efficiently, suggesting that DNMT3b3 also may be capable of DNA binding. Moreover, *de novo* methylation of *D4Z4* in T24 cancer cells after 5-Aza-CdR treatment only occurred when DNMT3b3 was expressed, reinforcing its role as a contributing factor of DNA methylation. The expression of either DNMT3b2 or 3b3, however, was not sufficient to explain the abnormal methylation of DNMT3b target sequences in human cancers, which may therefore be dependent on factors that affect DNMT3b targeting. Methylation analyses of immunodeficiency, chromosomal instabilities, and facial abnormalities cells revealed that an Alu repeat sequence was highly methylated, suggesting that Alu sequences are not DNMT3b targets.

Received 9/23/03; revised 11/17/03; accepted 11/24/03
The costs of publication of this article were defrayed in part by the payment of page charges. This article must therefore be hereby marked advertisement in accordance with 18 U.S.C. Section 1734 solely to indicate this fact.
Grant support: NIH grants CA 82422 and 1RO1 CA 83867 (P. A. J.), NIH Training Grant T32 DE07211-11 (M. V.), and NIH Training Grant in Basic Research in Oncology T32 CA09659 (D. W.).
Note: D. J. Weisenberger and M. Velicescu contributed equally to this work.
Requests for reprints: Peter A. Jones, University of Southern California/Norris Comprehensive Cancer Center and Hospital, 1441 Eastlake Avenue, Room 8302L, Mail Stop 83, Los Angeles, CA 90089-9181. Phone: (323) 865-0816; Fax: (323) 865-0102. E-mail: jones_p@ccnt.hsc.usc.edu

Introduction

Cytosine methylation is an essential process involved in mammalian embryonic development, X-chromosome inactivation, genomic imprinting, regulation of gene expression, and chromatin structure (for recent reviews, see Refs. 1, 2). DNA methylation patterns are established in a *de novo* fashion early during embryonic development and are maintained with each round of cell division. DNA methylation occurs at the C-5 position of cytosine in the context of the CpG dinucleotide (3) and is performed by at least three DNA methyltransferases (DNMT; 1, 3a, and 3b). These enzymes have different substrate specificities *in vitro* and are thought to have different methylation activities *in vivo*.

DNMT1 has a preference toward hemimethylated DNA (4–6), suggesting that it has maintenance activity and is responsible for copying the DNA methylation pattern on newly synthesized DNA. Mutations in the murine *Dnmt1* gene result in global hypomethylation and lethality in *Dnmt1* knockout mice (7). DNMT3a and 3b are thought to function as *de novo* DNMTs and the murine enzymes are required for *de novo* methylation after embryonic implantation as well as the *de novo* methylation of newly integrated retroviral sequences (8, 9). These enzymes were shown to have equal preferences *in vitro* for unmethylated and hemimethylated DNA (10). Similar to *Dnmt1*−/− mice, mouse knockouts of *Dnmt3a* and *3b* are also lethal (8). DNMT3a also methylates non-CpG sequences (11, 12) and can function as a transcriptional corepressor (13, 14). DNMT3b is required for the methylation of centromeric satellite repetitive elements and transcriptional repression (8, 14). Mutations in human *DNMT3b* have been shown to cause immunodeficiency, chromosomal instabilities, and facial abnormalities (ICF) syndrome (8, 15, 16). Recent studies have shown that DNMTs function in cooperation with each other to facilitate DNA methylation in both human and mouse systems (17–19).

All DNMT proteins contain highly conserved COOH-terminal catalytic domains while their NH_2-terminal regions are quite distinct. The NH_2-terminal regulatory domain of each DNMT is thought to direct nuclear localization and mediate interactions with other proteins. The COOH-terminal catalytic domains of DNMT contain several highly conserved motifs important for their enzymatic catalysis (motifs IV and VI), DNA binding (motif IX), and *S*-adenosylmethionine cofactor binding (motifs I and X; 20). Studies of prokaryotic (cytosine-5) DNMT have shown motif VIII to be also highly conserved (21–23) and a part of the core catalytic active site together with motifs IV and VI (21). However, the absolute requirement of

motif VIII for the catalytic activity of mammalian DNMT has not been shown. The nonconserved region between motifs VIII and IX represents the target recognition domain (TRD) that may be responsible for sequence specificity (21–23).

Unlike DNMT1 and 3a, DNMT3b is the only DNMT that is expressed as alternatively spliced variants that affect the integrity of the catalytic domain (10, 24–26). Among these, DNMT3b1 and 3b2 both contain all of the highly conserved motifs (I, IV, VI, VIII, IX, and X) as well as the TRD in the catalytic domain, but the DNMT3b2 variant lacks exons 10 and 11 (10, 25). Human and murine DNMT3b3 and murine Dnmt3b6 lack the less conserved motif VII, the more conserved motif VIII, the TRD, and the nine amino acids of motif IX (24). DNMT3b3 and Dnmt3b6 only differ in that exons 10 and 11 are absent in DNMT3b3 while they are present in Dnmt3b6 (26). Recently, it has been suggested that while murine Dnmt3b3 is catalytically inactive both *in vitro* (27) and *in vivo* (28), the human DNMT3b3 isoform was capable of methyl transfer (29). The specific roles of individual DNMT3b splice variants are not fully understood; however, DNMT3b isoforms are overexpressed in a variety of human cancers (24, 30). More recently, DNMT3b4 has been suggested to function as a negative regulator of DNA methylation in hepatocellular carcinoma cells despite its lack of catalytic activity (30). Gene targeting experiments have shown that DNMT3b plays an important role in the hypermethylation of CpG islands in human cancers (18) as well as in the maintenance methylation of repetitive elements in mouse cells (17). However, the role of DNMT3b in the aberrant methylation of CpG islands in human cancers is unclear, as a recent study by Robert *et al.* (31) showed that DNMT1 alone may be sufficient for the methylation of these sequences in cancer cells.

The goal of this study was to understand the biological significance of DNMT3b2 and 3b3 in the methylation of DNMT3b target sequences. We first identified new murine Dnmt3b isoforms and showed that embryonic stem (ES) cells only express isoforms that contain the conserved exons 10 and 11. We next showed by Western blot analysis that while DNMT1, 3a, 3b1, and 3b2 were completely depleted after treatment of mouse and human cells with 5-aza-2′-deoxycytidine (5-Aza-CdR), DNMT3b3 and Dnmt3b6 were also depleted although less efficiently, suggesting that these enzymes may interact with DNA and therefore may be involved in DNA methylation. This was reinforced by the findings that the *D4Z4* repeat as well as satellites 2 and 3 repetitive elements, which are all targets of DNMT3b, were methylated in cells that predominantly express DNMT3b3. However, despite the presence of DNMT3b2 and/or 3b3 in human cancer cells, hypomethylation of the satellite repeat sequences as well as hypermethylation of the CpG islands in the *p16* gene were detected, suggesting that the abnormal methylation of DNMT3b target sequences in human cancers is dependent on other factors that affect DNMT3b2 or 3b3 activity.

Results

Identification of Dnmt3b Splice Variants in Mouse ES and Somatic Cells

DNMT3b splice variants are highly conserved between human and mouse (10, 24). Six Dnmt3b isoforms have been described in the mouse: Dnmt3b1, 3b2, 3b3, 3b4, 3b5, and 3b6 (10, 26, 28, 29). While Dnmt3b1 is encoded by a full-length mRNA, Dnmt3b2 is generated by alternative splicing at exons 10 and 11. Dnmt3b6 is missing exons 21 and 22 in the catalytic domain, while Dnmt3b3 is characterized by splicing at both exons 10 and 11 and exons 21 and 22 (10, 26). Human DNMT3b1, 3b2, and 3b3 have also been previously characterized (24, 25) as well as two additional splice variants DNMT3b4 and 3b5 (24). Exons 21 and 22 are removed from DNMT3b4 and 3b5, respectively (24).

Additional Genbank submissions (accession nos. AF151972, AF151973, AF151974, and AF151975) suggested that mouse cells contain additional Dnmt3b mRNA splice variants that were not previously characterized. These mRNA sequences differed from the previous described Dnmt3b transcripts in that these sequences harbored an additional splicing event that removed 114 nucleotides upstream of the ATG translation start site in exon 2 (5′ end). Because this splicing event would not alter the protein sequence, it represents an alternative 5′ untranslated region (UTR).

We performed semiquantitative reverse transcription-PCR (RT-PCR) analysis on ES, 10T1/2, NIH3T3, and MEF cells using primers that flanked the potential splice sites: 5′ end (exon 2), exons 10 and 11, and the catalytic domain (exons 21 and 22; Fig. 1A). Splicing events at the 5′ end and the catalytic domain were detected in ES cells, whereas the splicing event at exons 10 and 11 was not observed (Fig. 1A). Splicing events at the 5′ end, exons 10 and 11, and exons 20–22 (catalytic domain) were identified in all three somatic cell lines. The presence of exons 10 and 11 in Dnmt3b mRNA transcripts in ES cells suggests that this region may be required for normal embryonic development or may be specific for undifferentiated cells. The presence of multiple bands in the RT-PCR analysis of the catalytic domain of mouse cell lines suggested the existence of Dnmt3b1, 3b2, 3b3, 3b4, 3b5, and 3b6 splice variants (28, 29). The combined splicing events create 16 possible Dnmt3b mRNA species in the mouse (Fig. 1B). The mRNA species in which the 5′ end splicing event occurred were designated as *U* (5′ UTR). Interestingly, ES cells expressed Dnmt3b mRNAs that contain exons 10 and 11, while the Dnmt3b mRNA expression in the mouse somatic cell lines was characterized by the absence of these exons (Fig. 1, A and B). Because Dnmt3b4 and 3b5 mRNAs are characterized by the absence of exons 10 and 11, we designated these mRNA species in ES cells as Dnmt3b7 and 3b8, respectively, along with their accompanying *U* isoforms (Fig. 1B).

Using primers specific for the 5′ end and catalytic domain splicing events, we amplified full-length Dnmt3b mRNAs by RT-PCR, and their identities were confirmed by DNA sequencing (data not shown). Based on the RT-PCR analysis, ES cells expressed seven Dnmt3b mRNA isoforms, all of which contain exons 10 and 11 (Dnmt3b1, 3b6, and 3b7), as well as the *U* isoforms for Dnmt3b1, 3b6, 3b7, and 3b8. Somatic cells expressed seven mRNA splice variants that lack exons 10 and 11 (Dnmt3b2, 3b3, and 3b4) and the *U* isoforms of Dnmt3b2, 3b3, 3b4, and 3b5 (Fig. 1B). However, Dnmt3b5 and 3b8 were not successfully amplified by RT-PCR. Because Dnmt3b5 has been previously characterized (28, 29), Dnmt3b5 and/or 3b8 may be expressed at levels undetectable by RT-PCR or in other

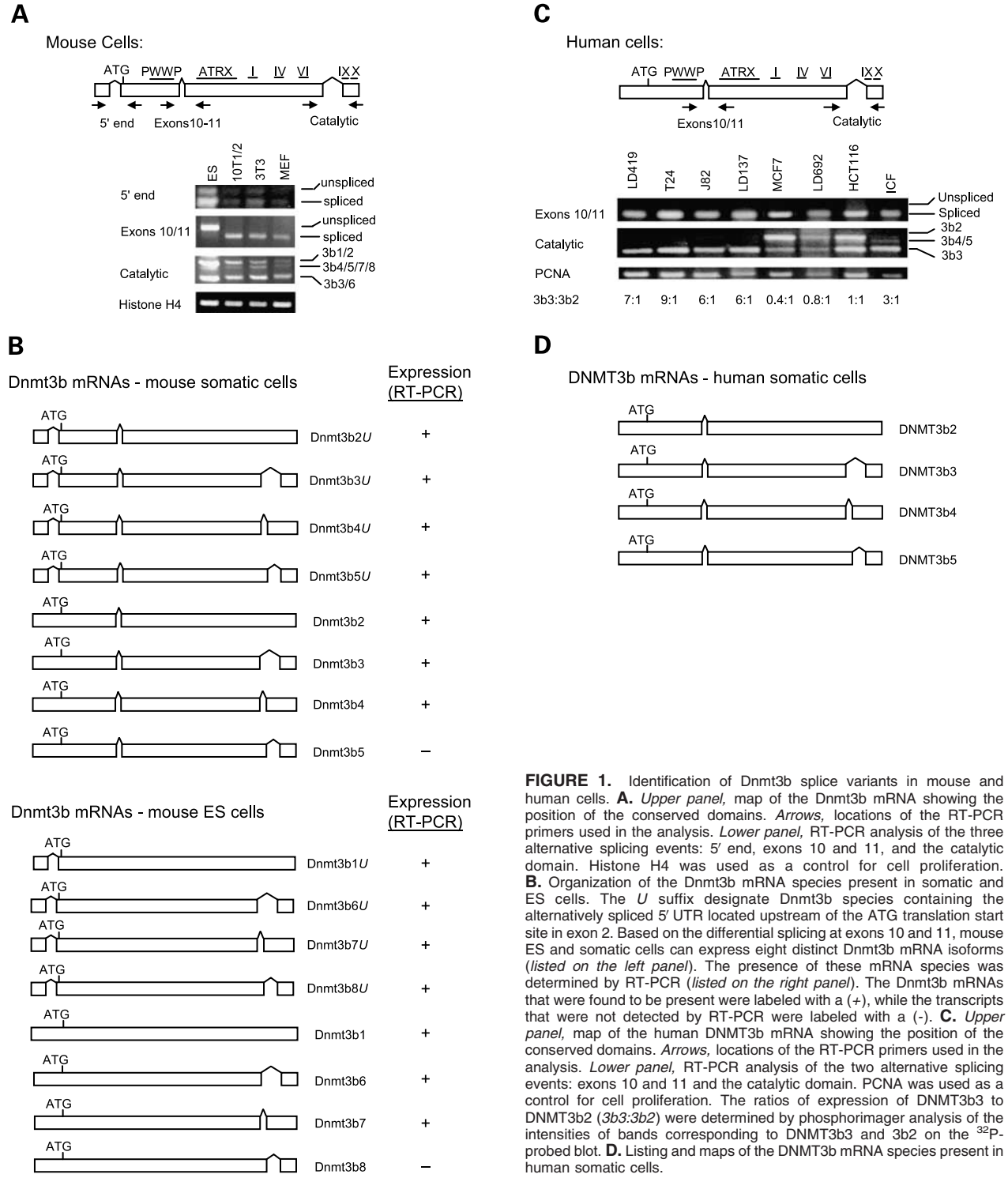

FIGURE 1. Identification of Dnmt3b splice variants in mouse and human cells. **A.** *Upper panel,* map of the Dnmt3b mRNA showing the position of the conserved domains. *Arrows,* locations of the RT-PCR primers used in the analysis. *Lower panel,* RT-PCR analysis of the three alternative splicing events: 5′ end, exons 10 and 11, and the catalytic domain. Histone H4 was used as a control for cell proliferation. **B.** Organization of the Dnmt3b mRNA species present in somatic and ES cells. The *U* suffix designate Dnmt3b species containing the alternatively spliced 5′ UTR located upstream of the ATG translation start site in exon 2. Based on the differential splicing at exons 10 and 11, mouse ES and somatic cells can express eight distinct Dnmt3b mRNA isoforms (*listed on the left panel*). The presence of these mRNA species was determined by RT-PCR (*listed on the right panel*). The Dnmt3b mRNAs that were found to be present were labeled with a (+), while the transcripts that were not detected by RT-PCR were labeled with a (-). **C.** *Upper panel,* map of the human DNMT3b mRNA showing the position of the conserved domains. *Arrows,* locations of the RT-PCR primers used in the analysis. *Lower panel,* RT-PCR analysis of the two alternative splicing events: exons 10 and 11 and the catalytic domain. PCNA was used as a control for cell proliferation. The ratios of expression of DNMT3b3 to DNMT3b2 (*3b3:3b2*) were determined by phosphorimager analysis of the intensities of bands corresponding to DNMT3b3 and 3b2 on the ^{32}P-probed blot. **D.** Listing and maps of the DNMT3b mRNA species present in human somatic cells.

tissues not included in this analysis. In addition, Dnmt3b*5U* and 3b*8U* mRNAs were detected, suggesting that Dnmt3b5 and 3b8 proteins may be present because these *U* mRNA isoforms do not change the coding sequence.

For comparison, we also performed RT-PCR analyses of DNMT3b splice variants in several human cell lines using primers that flanked exons 10 and 11 and exons 21 and 22 of the catalytic domain (Fig. 1C). Similar to the mouse somatic cells, all of the human cell lines analyzed lacked exons 10 and 11, suggesting that DNMT3b2, but not DNMT3b1, is expressed in human somatic cells (Fig. 1C). Analysis of the catalytic domain identified the presence of DNMT3b2 and 3b3, while

DNMT3b4 and/or 3b5 mRNAs were only detected at very low levels (Fig. 1, C and D). Normal LD419 fibroblasts, T24, J82, LD137, and LD692 bladder cancer cells, and ICF fibroblasts expressed predominantly DNMT3b3 mRNA along with very low levels of DNMT3b2 (Fig. 1C). Analysis of the RT-PCR products by semiquantitative methods revealed a 7:1 ratio of DNMT3b3 to DNMT3b2 in LD419 cells, a 9:1 ratio in T24 cells, and a 6:1 ratio in J82 and LD137 cells. MCF7 cells expressed DNMT3b2 and to a lesser extent DNMT3b3 mRNA while LD692 and HCT116 cells expressed DNMT3b2 and 3b3 transcripts approximately at the same levels (Fig. 1C). The expression levels of DNMT1 and 3a mRNA were similar in the human cells analyzed (data not shown).

Depletion of Murine Dnmt Proteins After Treatment of ES Cells With 5-Aza-CdR

We next tested the specificities of the antibodies against murine Dnmts for use in Western blot analysis in wild-type and knockout mouse ES cells (7, 10, 32). The wild-type ES cells were previously shown to express Dnmt3b mRNA at significantly higher levels compared with somatic mouse cell types (10). The antibodies detected proteins for Dnmt1, Dnmt3a, and two proteins for Dnmt3b, which were previously identified as Dnmt3b1 and 3b6 (Fig. 2A; 26). ES cell knockouts of *Dnmt3a* (M1 and M1/3B cells) and *3b* (M1 and M1/3A cells) showed complete loss of Dnmt3a and 3b proteins, respectively (Fig. 2A). No cross-reactivity between Dnmt proteins was seen in these experiments. However, a minor signal was detected for Dnmt1 in the *Dnmt1*−/− cells (3A/3B cells; Fig. 2A). A similar band was seen in protein lysates from a second *Dnmt1*−/− cell line (32; data not shown). Because this band was only weakly present, it was considered as background cross-reactivity.

While Dnmt3b1 and 3b2 proteins have been shown to be catalytically active (27), Dnmt3b3 and 3b6 were suggested to be catalytically inactive (26–28). As Dnmt3b4 and 3b5 proteins are similar to their human homologues, it is most likely that they are also catalytically inactive. Because ES cells expressed predominantly Dnmt3b1 and 3b6 proteins (Fig. 2A; 26), we developed a Western blot-based assay to compare the degree of depletion of these murine splice variants as well as Dnmt1 and 3a proteins after treatment with the demethylating agent 5-Aza-CdR. The mechanism of 5-Aza-CdR-induced demethylation is thought to be due to covalent trapping of the DNMT to the azacytosine base (33–35). We reasoned that if the DNMT could bind through the conserved motifs in the catalytic domain, trapping of the enzyme to the modified DNA would occur, and the free enzyme would not be detected in a total protein cell lysate. Wild-type ES cells were treated with 5-Aza-CdR for 24 h, and protein cell lysates under treated and untreated conditions were isolated 1 day after the initial treatment. Western blot analyses showed a complete depletion of Dnmt1, 3a, and 3b1 proteins and to a lesser extent 3b6 protein after 5-Aza-CdR treatment (Fig. 2B). Dnmt1, 3a, 3b1, and 3b2 proteins all contain a complete catalytic domain, whereas catalytic motifs VII and VIII and the first nine amino acids of motif IX are absent in Dnmt3b3 and 3b6. These results indicate that despite the absence of these motifs, Dnmt3b3 and 3b6 proteins may indeed bind to azacytosine-containing DNA. Dnmt mRNA transcripts were not significantly reduced following drug treatments when compared with the S-phase specific marker histone H4 (H4F2) as detected by semiquantitative RT-PCR (Fig. 2C), supporting the idea that the reduction in Dnmt protein levels was due to trapping of the enzymes to the azacytosine-incorporated DNA rather than an inhibition of transcription or cell proliferation.

Effects of 5-Aza-CdR on Human DNMT3b Protein Levels

We then compared the protein expression of DNMTs in seven human cell lines by Western blot analysis. DNMT1 was appreciably expressed in all the human cell lines (Fig. 3A).

Similar to the RT-PCR results of DNMT3b isoforms in human cells, the expression of DNMT3b2 and/or 3b3 proteins in the human cell lines showed that DNMT3b3 protein was

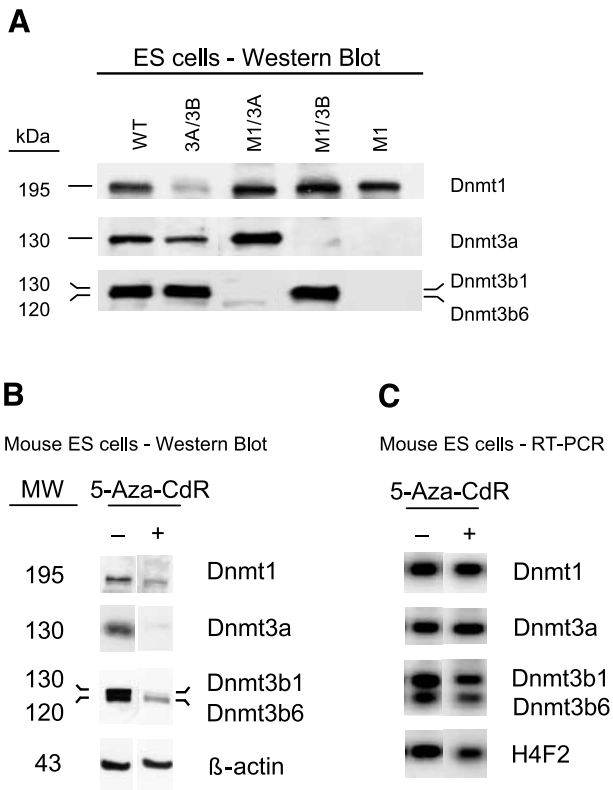

FIGURE 2. Depletion of murine Dnmt proteins after 5-Aza-CdR treatment. **A.** Dnmt protein levels in wild-type (M1/3A/3B; *WT*) ES cells and *Dnmt1*−/− (*3A/3B*), *3b*−/− (*M1/3A*), *3a*−/− (*M1/3B*), and *3a/3b*−/− (*M1*) knockout ES cells. Equal amounts (30 μg) of protein extracts were analyzed by SDS-PAGE, and Dnmt proteins were identified using antibodies specific for each Dnmt protein. The *two bands* identified by the Dnmt3b antibody represent the alternatively spliced variants Dnmt3b1 and 3b6. **B.** Western blot of Dnmt protein levels in mouse ES cells under untreated conditions or after treatment with 5-Aza-CdR. Protein cell lysates were collected from untreated and 5-Aza-CdR-treated cells 24 h after the initial drug treatment. Expression levels of β-actin were determined to confirm accurate protein loading. **C.** Semiquantitative RT-PCR of Dnmt mRNA levels in ES cells under untreated or treated conditions. H4F2 was used as a marker for cell proliferation.

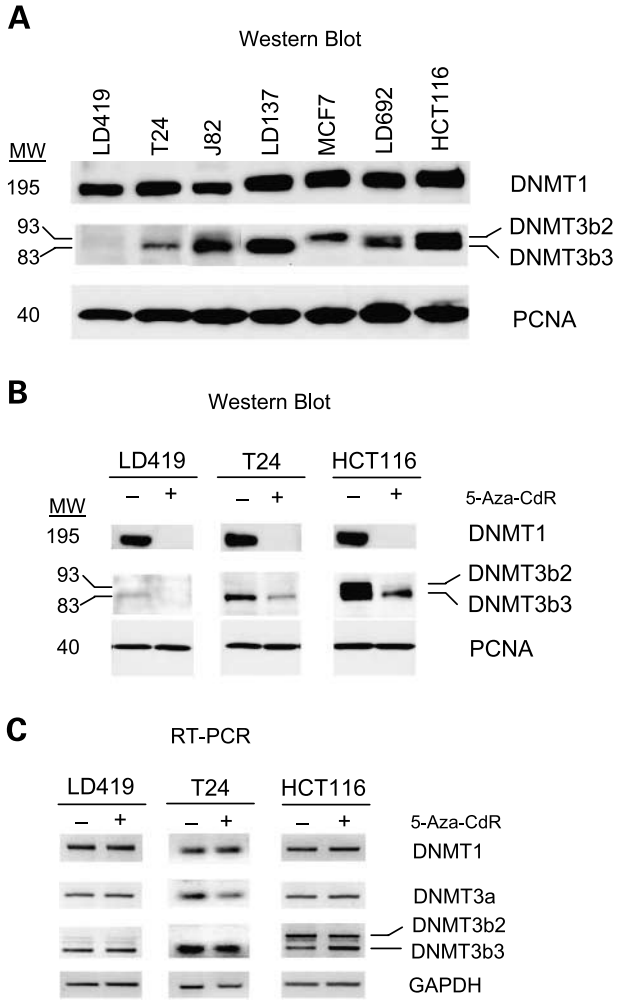

FIGURE 3. Depletion of DNMT proteins after 5-Aza-CdR treatment of human cell lines. **A.** DNMT1 and 3b protein levels in seven human cell lines. PCNA was used as a marker of cell proliferation. **B.** Depletion of DNMT1 and 3b proteins after 5-Aza-CdR treatment of LD419, T24, and HCT116 cells. Protein cell lysates were collected from untreated and 3 μM 5-Aza-CdR-treated cells 24 h after the initial drug treatment. PCNA was used as a control for cell proliferation in the Western blot analyses. **C.** Semiquantitative RT-PCR of DNMT mRNA levels in LD419, T24, and HCT116 cells under untreated or treated conditions. Glyceraldehyde-3-phosphate dehydrogenase (*GAPDH*) was used as a loading control.

weakly detected in LD419, T24, J82, and LD137 cells. DNMT3b2 was highly expressed in MCF7 cells, while LD692 and HCT116 cells expressed DNMT3b2 and 3b3 proteins equally (Fig. 3A). DNMT1 and 3b proteins were barely detectable in ICF cells even when 100 μg of total protein were used (data not shown). This was most probably due to a lower rate of cell proliferation because the mRNAs for these proteins are highly cell cycle regulated (36). DNMT3a protein levels could not be determined because reliable antibodies were not available commercially.

We next compared the extent of changes in DNMT1 and 3b3 protein levels after 5-Aza-CdR treatment of LD419 normal human bladder fibroblasts as well as T24 and HCT116 cancer cells. Western blot analyses indicated that DNMT1 proteins were completely depleted after treatment (Fig. 3B). Following treatment of these cells with 5-Aza-CdR, DNMT3b3 protein was mildly depleted in T24 cells but completely depleted in LD419 cells (Fig. 3B). HCT116 cells, which equally expressed DNMT3b2 and 3b3 proteins, showed a mild reduction of DNMT3b3 while DNMT3b2 was completely depleted (Fig. 3B). The limited reduction of human DNMT3b3 protein levels following drug treatment of T24 and HCT116 cells was similar to that of murine Dnmt3b6 in ES cells (Fig. 2B). Both of these variants are characterized by the deletion of exons 21 and 22. The complete reduction of DNMT3b3 in LD419 cells after drug treatment may be attributed to the lower basal level of expression of DNMT3b3 protein in LD419 cells than in the cancer cells (Fig. 3B). Similar to the mouse experiment, DNMT1, 3a, 3b2, and 3b3 mRNA levels were not affected by drug treatment (Fig. 3C), further suggesting that the reduction of DNMT proteins following 5-Aza-CdR treatment was not due to transcriptional inhibition but rather to the trapping of the enzyme to azacytosine-substituted DNA.

Role of DNMT3b3 in de novo Methylation of the D4Z4 Subtelomeric Repeat Sequence

The nearly 9-fold increased expression of DNMT3b3 mRNA relative to DNMT3b2 mRNA in T24 cells led us to further investigate whether *de novo* methylation of a DNMT3b target sequence can occur in these cells. We first measured the methylation of the *D4Z4* subtelomeric repetitive element by methylation-sensitive single nucleotide primer extension (Ms-SNuPE). This repeat sequence was recently shown to be hypomethylated in ICF cells (37), which are characterized by mutations in the *DNMT3b* gene (8, 15, 16). The high level of methylation of *D4Z4* in T24 cells (~80%; day 0; Fig. 4) showed that the methylation of this DNMT3b target sequence was not compromised in cells that predominantly express DNMT3b3.

We next assessed whether *D4Z4* can become *de novo* methylated after treatment of T24 cells with 5-Aza-CdR. Cells were treated with 5-Aza-CdR for 24 h, as previously described (38, 39), and then allowed to grow to confluence by day 3, the time point at which maximum demethylation of *D4Z4* occurred (Fig. 4). After this time, some cells were maintained in a nondividing state by serum starvation and confluence, while duplicate cultures were allowed to proliferate. Treatment with 5-Aza-CdR caused a strong demethylation of *D4Z4* at day 3 (Fig. 4). *D4Z4* became remethylated in a *de novo* fashion by day 20 after treatment in dividing cells while only low levels of *D4Z4* remethylation (<15%) were detected in cells that were prevented from dividing after drug treatment (Fig. 4). We previously showed that under these experimental conditions, the *p16* promoter underwent *de novo* remethylation only in dividing cells. DNMT3b3 protein was present in dividing cells but absent in the nondividing cells. Moreover, DNMT3b3 protein levels increased from days 6 to 20 in dividing T24 cells as these cells recovered from 5-Aza-CdR treatment. However, DNMT3b3 protein remained absent in cells that were prevented from dividing over this same time period after drug treatment (38). These data suggest that *de novo* methylation of *D4Z4* also occurred in the dividing cells that express DNMT3b3 but not in

cells in which DNMT3b3 was absent. This correlates with a requirement of DNMT3b3 for the *de novo* methylation of *D4Z4*. Although DNMT1 exhibited a similar pattern of expression as DNMT3b3 in this experiment (38), its contribution for *de novo* methylation of this specific DNMT3b target sequence is not known.

Correlation Between Human DNMT3b Splice Variant Expression and the DNA Methylation of DNMT3b Target Sequences

DNMT3b3 mRNA is preferentially expressed in several human tissues (24). Because DNMT3b3 protein appeared to be required for the methylation of *D4Z4* in T24 cells, we next selected several human cell lines that differed in the type of DMNT3b splice variant expressed to compare the methylation of DNMT3b target sequences. DNMT3b3 mRNA and protein was the predominant isoform expressed in ICF, LD419, T24, J82, LD137, and LD692 cells, while significant levels of both DNMT3b2 and 3b3 mRNA and protein were detectable in MCF7 and HCT116 cells (Figs. 1C and 3A).

We measured the methylation levels of several known DNMT3b target sequences: satellites 2 and 3 repeat sequences, *D4Z4*, *p16* promoter, and *p16* exon 2. Satellites 2 and 3 and *D4Z4* repeats are methylated in normal cells, while the *p16* promoter and *p16* exon 2 have been shown to be hypermethylated by the combined efforts of DNMT1 and 3b proteins in numerous human cancers (40). We also included an Alu repeat sequence in the *p53* gene, which is methylated in all human tissues (41). Satellites 2 and 3 were hypomethylated in ICF fibroblasts but were methylated in LD419 fibroblasts that expressed predominantly DNMT3b3 mRNA and protein. These satellite repeats, however, were hypomethylated in the majority of tumor cell lines irrespective of the expression of DNMT3b2 or 3b3 protein. Moreover, these repeats were methylated in HCT116 colon cancer cells, which expressed both DNMT3b2 and 3b3 proteins equally (Figs. 3A and 5A). Therefore, the expression of either DNMT3b2 or 3b3 protein in the tumor cell lines could not rescue the methylation of the satellite sequences.

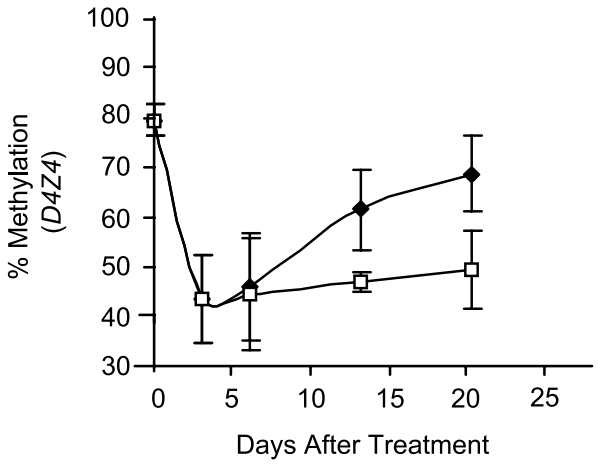

FIGURE 4. Kinetics of *D4Z4* remethylation after treatment of T24 cells with 5-Aza-CdR. Cells were treated with 5-Aza-CdR and then allowed to either divide or maintained in a nondividing state after removal of the drug. Genomic DNA was isolated at various time points, treated with bisulfite, and then subjected to Ms-SNuPE analysis. *Points,* percent methylation over the time course (average of three experimental trials); *bars,* SD. *Filled diamonds,* dividing cells; *open squares,* nondividing cells.

D4Z4 was unmethylated in ICF cells, ~50% methylated in LD419 normal bladder fibroblasts, and hypermethylated in all the tumor cell lines analyzed (Fig. 5B). The methylation of *D4Z4* and the satellite repetitive elements in LD419 cells, in which DNMT3b3 mRNA and protein is predominantly expressed, suggests that DNMT3b3 is required for the methylation of these sequences.

The CpG islands in the *p16* promoter (Fig. 5C) and exon 2 (Fig. 5D) were unmethylated in ICF and LD419 cells and were differentially methylated in the tumor cell lines analyzed. The *p16* promoter was unmethylated while the *p16* exon 2 was highly methylated in J82 bladder cancer cells, which expressed DNMT3b3 protein exclusively (Figs. 3A and 5, C and D). Both CpG islands were completely methylated in T24 cells, which predominantly expressed DNMT3b3. These CpG islands were also differentially methylated in tumor cells that expressed both DNMT3b2 and 3b3 proteins (LD137, MCF7, LD692, and HCT116). The *p16* exon 2 CpG island was highly methylated in every tumor cell line analyzed; however, the *p16* promoter CpG island was unmethylated in LD137 cells and 50–90% methylated in MCF7, LD692, and HCT116 cells (Fig. 5C).

These data suggest that other *trans*-acting factors may be responsible for modulating DNMT3b activity in cancer cells. The Alu repeat in the *p53* gene was completely methylated in all cell lines analyzed, including ICF cells (Fig. 5E), suggesting that this sequence is not a methylation target of DNMT3b. The combined methylation and DNMT3b mRNA expression data (Fig. 5F) suggested that the methylation of DNMT3b target sequences occurred in normal cells that express predominantly DNMT3b3. The expression of DNMT3b2 or 3b3 proteins, however, was not sufficient to explain the aberrant methylation of DNMT3b target sequences in human tumor cells.

Discussion

DNMT3b is a *de novo* DNMT that has numerous alternatively spliced variants including some with compromised catalytic activity (24, 30). In this study, we identified additional murine Dnmt3b mRNA isoforms (Dnmt3b7 and 3b8), which, based on their similarities with the human DNMT3b4 and 3b5 homologues, may also be catalytically inactive. The identification of distinct Dnmt3b variants present in murine ES and somatic cells demonstrated their possible involvement during embryonic development. Exons 10 and 11 containing mRNA transcripts were shown to be present in ES cells but absent in the somatic cells analyzed in this study. This region of Dnmt3b is between the Pro-Trp-Trp-Pro and the cysteine-rich plant homeodomain-like domains of the enzyme (42) and therefore may be an important structural moiety, but its role in Dnmt3b enzymology in ES cells and embryonic development is not understood. One interesting possibility may involve the

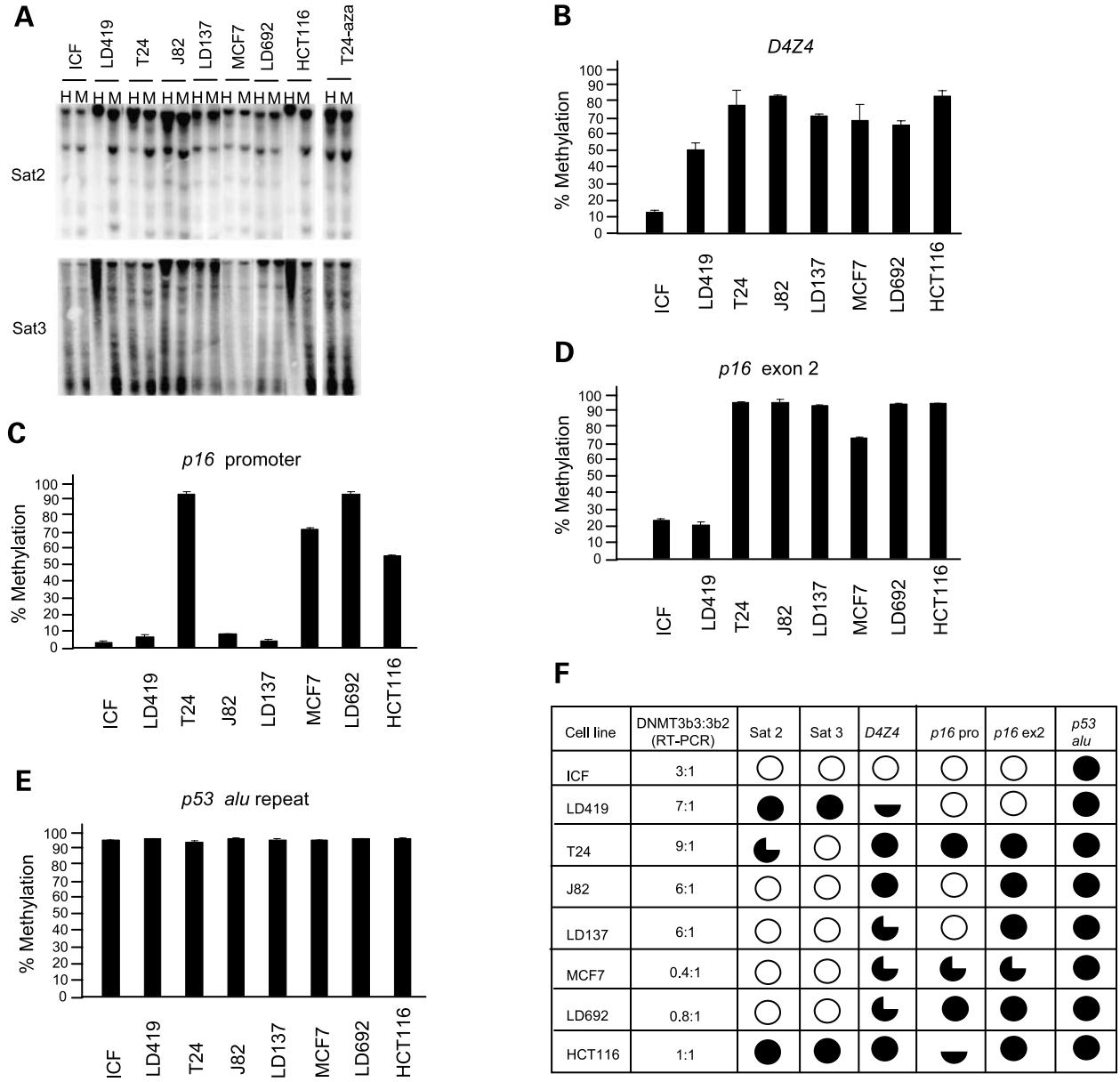

Cell line	DNMT3b3:3b2 (RT-PCR)	Sat 2	Sat 3	*D4Z4*	*p16* pro	*p16* ex2	*p53 alu*
ICF	3:1	○	○	○	○	○	●
LD419	7:1	●	●	◒	○	○	●
T24	9:1	◔	○	●	●	●	●
J82	6:1	○	○	●	○	●	●
LD137	6:1	○	○	◔	○	●	●
MCF7	0.4:1	○	○	◔	◔	◔	●
LD692	0.8:1	○	○	◔	●	●	●
HCT116	1:1	●	●	●	◒	●	●

FIGURE 5. DNA methylation levels of DNMT3b target sequences in human cell lines. **A.** Methylation status of satellites 2 and 3 repetitive elements measured by Southern blot analysis. Methylation levels of (**B**) *D4Z4*, (**C**) *p16* promoter, (**D**) *p16* exon 2, and (**E**) *p53* Alu repeat sequence were measured by Ms-SNuPE analysis. *Columns,* mean; *bars,* SD. **F.** Combined methylation data from **A** to **E**. The major DNMT3b splice variant expressed and the methylation status are provided for each cell line. *Open circles,* an unmethylated DNA sequence; *filled circles,* methylated sequences; *half circles,* a region that is ~50% methylated; *three-fourth circles,* a region that is ~75% methylated.

requirement of the amino acid sequence encoded by exons 10 and 11 in recruiting proteins involved in chromatin structure modification and reorganization. This region lies in the NH_2 terminus of the Dnmt3b protein, which is involved in transcriptional regulation (14).

We also showed that the human DNMT3b3 protein may be required for the methylation of its target sequences. However, its catalytic activity remains controversial. A recent study showed that human DNMT3b3 possesses catalytic activity (29) and is in contrast to reports suggesting that murine Dnmt3b3 and 3b6 proteins were catalytically inactive *in vitro* (27) and *in vivo* (28). Our studies showed that DNMT3b3 was the predominant DNMT3b isoform expressed in normal LD419 fibroblasts and T24 bladder cancer cells in which the known DNMT3b target, *D4Z4*, was methylated. Furthermore, *D4Z4* became *de novo* methylated following treatment of T24 cells with 5-Aza-CdR when DNMT3b3 protein was expressed, suggesting that DNMT3b3 was also required for *de novo* methylation of this sequence. Although these data are correlative, our results highlight a potentially important role of DNMT3b3 that will require future investigation.

The partial depletion of human DNMT3b3 and mouse Dnmt3b6 proteins after 5-Aza-CdR treatment further supports the idea that these enzymes interact with DNA and provide more evidence of their importance in DNA methylation. The 5-Aza-CdR-mediated depletion of DNMT3b3 and 3b6 proteins may be facilitated by the highly conserved motifs that are thought to mediate the enzymatic activity of methyl transfer (20). Human and murine DNMT1, 3a, and 3b1/2 proteins contain 10 conserved catalytic domain motifs (I–X) as well as the nonconserved TRD domain. Human DNMT3b3 and murine Dnmt3b3/6 proteins are characterized by deletions of motifs VII and VIII, the TRD, and the first nine amino acids of motif IX.

Experiments performed using catalytically incompetent mutant bacterial (cytosine-5) DNMT showed that the formation of the covalent complex between the enzyme and the azacytosine-substituted DNA is mediated by the conserved cysteine-proline doublet in motif IV (41–48). Because DNMT3b3 and 3b3/6 proteins contain these amino acids, these isoforms might be capable of forming a covalent complex with aza-modified DNA. The less conserved motif VIII has been shown to form the catalytic core of bacterial DNMT m*Hha*I together with motifs IV and VI (22). However, the absolute requirement of motif VIII for proper enzyme activity in mammalian cells has not been shown. In addition, the function of motif VII in mammalian DNMTs is unclear. The absence of the TRD and a portion of motif IX in human DNMT3b3 and murine Dnmt3b3/6 proteins may affect their sequence specificities and/or DNA binding affinities. However, the remaining amino acids of motif IX may allow the enzyme to weakly bind the substrate and as a result its limited depletion by 5-Aza-CdR. A recent study (49) has shown that the bacterial DNMT m*Hha*I can form covalent complexes with aza-modified DNA *in vitro* in both the absence and the presence of the *S*-adenosylmethionine cofactor, suggesting that the methyl transfer step may follow the inhibition by aza-modified DNA. The relevance of this finding to the mammalian system is not yet known.

Despite the controversy regarding its methyl transfer capabilities, DNMT3b3 may still function as a positive regulator of DNA methylation. This is not unprecedented, as a recent study has shown that the catalytically inactive DNMT3b4 variant may act as a dominant-negative regulator of DNA methylation in human hepatocellular carcinomas (30). Similarly, Dnmt3L is required for the *de novo* methylation of imprinted DNA sequences and is thought to function as a regulator rather than as a DNMT (50).

DNMT3b3 may also function in cooperation with another DNMT, such as DNMT1. In this scenario, DNMT3b3 may serve to target or tether DNMT1 to a locus to be methylated. This is consistent with recent work from our laboratory showing that Dnmt1 functions in a cooperative manner with Dnmt3a and/or 3b to facilitate maintenance DNA methylation (17). Recent studies have also described interactions among human DNMT1, 3a, and 3b proteins (19) as well as the interactions among murine Dnmt3a, 3b and 3L in ES cells (51). A recent study has also shown that DNMT3L facilitates *de novo* methylation specifically by Dnmt3a but not by DNMT3b (52), suggesting that DNMT3b3 may also specifically interact with other DNMTs to facilitate DNA methylation.

DNMT3b, in cooperation with DNMT1, plays a role in the aberrant hypermethylation of CpG islands in cancer cells (18). Our study showed that other targets of DNMT3b, such as the *D4Z4* and satellites 2 and 3 repeat sequences, were also aberrantly methylated in human cancers. *D4Z4* was hypermethylated in all the human cancer cell lines analyzed, while the satellite repeats were hypomethylated in a large majority of these cells. The hypermethylation of *D4Z4* in the cancer cell lines used in this study further suggested that CpG islands are not the exclusive sites of DNA hypermethylation. Moreover, the high levels of methylation of an Alu repeat in ICF cells suggests that Alu sequences are not targets of DNMT3b. The near complete methylation of the Alu repeat in the cancer cells also shows that not all repetitive elements are targets of DNA hypomethylation in cancers. Identifying regions of DNA hypomethylation and hypermethylation of repetitive elements in human cancers may help to better understand these phenomena.

A recent study, however, has shown that DNMT1 alone may be responsible for the aberrant hypermethylation of CpG islands present in HCT116 cells (31) because DNMT1 alone was completely depleted by 5-Aza-CdR treatment while DNMT3a and 3b protein levels were not affected. Our results show a complete depletion of DNMT3b2 and a mild depletion of DNMT3b3 proteins in both mouse and human cell lines after a higher (3 μM) dose of 5-Aza-CdR. The discrepancy between the two studies may be due to differences in the concentration of 5-Aza-CdR as well as antibodies used to detect DNMT3b protein isoforms by Western blot analysis. Our results have been reproduced in both mouse and human cell systems, and the specificities of the antibodies have been confirmed in *Dnmt3b* −/− ES cells and are closely correlative to the DNMT3b mRNA species in human and mouse cells.

The expression of DNMT3b2 or 3b3 mRNA and protein in the human cell lines could not explain the differential methylation of DNMT3b target sequences. Because the overall DNMT3b mRNA expression levels were similar in the cancer cell lines as measured by semiquantitative RT-PCR, the hypomethylation and hypermethylation of DNMT3b target sequences may be explained by an improper targeting of the enzyme. The differential methylation of CpG islands in J82 and LD137 cancer cells, where the *p16* exon 2 CpG island was hypermethylated but the *p16* promoter remained unmethylated, also supports this hypothesis. Moreover, in HCT116 colon cancer cells, one allele of the *p16* promoter is completely methylated, while the second allele is unmethylated (53), and this further implies that DNMT3b targeting may be affected in cancer cells. The mechanism driving the process of *de novo* methylation is not known at this time. However, an aberrant targeting of DNMT3b protein isoforms may suggest that other factors related to gene transcription or chromatin remodeling may help designate regions of DNA methylation in cancer cells.

Materials and Methods

Cell Culture

Wild-type mouse ES cells as well as ES cells containing knockouts of *Dnmt3a*, *3b*, or *3a/3b* were obtained from Dr. En Li (Massachusetts General Hospital, Boston, MA). *Dnmt1*

knockout ES cells were obtained from Dr. Peter Laird (University of Southern California). All ES cells were cultured in the presence of irradiated mouse embryonic fibroblast feeder cells in Dulbecco's MEM supplemented with 15% non-heat-inactivated FCS, 20 mM HEPES buffer, and 1000 units/ml leukemia inhibitory factor. The T24 and HCT116 cells were obtained from the American Type Culture Collection (Rockville, MD). T24 and HCT116 cells were cultured in McCoy's 5A medium. All media were supplemented with 10% heat-inactivated FCS, 100 units/ml penicillin, and 100 μg/ml streptomycin. LD419 cells were isolated in our laboratory from human bladder embryonic fibroblasts and were cultured in McCoy's 5A medium supplemented with 20% heat-inactivated FCS, 100 units/ml penicillin, and 100 μg/ml streptomycin. J82, LD137, and LD692 cells were cultured as previously described (54). Mouse C3H/10T1/2/CL8 (10T1/2), NIH3T3, and MEF cells were cultured as described (55). ICF fibroblasts from Coriell Cell Repository (Camden, NJ; GM08747) were cultured as recommended by the supplier.

5-Aza-CdR Treatments

Mouse wild-type ES cells were plated (2×10^6 cells/60 mm dish) and were treated with 3×10^{-7} M 5-Aza-CdR 24 h later. RNA and protein extracts were collected from treated or untreated cells 24 h after the initial drug treatment. LD419, T24, and HCT116 cells were plated (1.5×10^6 cells/100 mm dish) and were treated with 3×10^{-6} M 5-Aza-CdR 24 h later. DNA, RNA, and protein extracts were collected from untreated and treated cells 24 h after the initial drug treatment. For *D4Z4* analysis, T24 cells were treated with 5-Aza-CdR as described previously (38).

Western Blot Analysis of Dnmt Protein Levels

Cells were rinsed twice with ice-cold PBS and lysed by the addition of radioimmunoprecipitation buffer (PBS, 0.1% SDS, 0.5% NP40, and 0.5% sodium deoxycholate). Cells were scraped off dishes and placed on ice for 30 min. The mixture was centrifuged at 13,000 rpm for 30 min at 4°C, and the supernatant was used for Western blot analysis. Approximately 30 μg total protein extract were loaded onto 4–15% gradient Tris-HCl gels (Bio-Rad, Hercules, CA), electrophoresed in Tris-glycine-SDS running buffer [25 mM Tris, 192 mM glycine, and 0.1% SDS (pH 8.3)], and transferred to polyvinylidene difluoride membranes in Tris-glycine buffer [25 mM Tris and 192 mM glycine (pH 8.2)] overnight at 4°C. The membranes were hybridized with antibodies against murine Dnmt1 (1:200 dilution; Santa Cruz Biotechnology, Santa Cruz, CA), murine Dnmt3a (1:750 dilution; Imgenex, San Diego, CA), murine Dnmt3b (1:750 dilution; Imgenex), human DNMT1 (1:1000 dilution; New England Biolabs, Beverly, MA), human DNMT3b (1:500 dilution; Santa Cruz Biotechnology), p16 (1:200 dilution; Santa Cruz Biotechnology), proliferating cell nuclear antigen (PCNA; 1:4000 dilution; Santa Cruz Biotechnology), and β-actin (1:2000 dilution; Sigma Chemical Co., St. Louis, MO) in Tris-buffered saline-Tween buffer (0.1 M Tris, 1.5 M NaCl, and 1% Tween 20) with 5% nonfat dry milk overnight at 4°C. The membranes were washed five times with Tris-buffered saline-Tween buffer at room temperature and incubated with secondary antibodies as follows: anti-mouse IgG-horseradish peroxidase (HRP; 1:2000 dilution for Dnmt3a and 3b, p16, PCNA, and β-actin; Santa Cruz Biotechnology), anti-goat IgG-HRP (1:10000 for Dnmt1 and DNMT3b; Santa Cruz Biotechnology), and anti-rabbit IgG-HRP (1:2000 dilution for DNMT1; Santa Cruz Biotechnology). All were incubated with the membrane for 1 h at room temperature. Proteins were detected with the enhanced chemiluminescence detection kit (Amersham-Pharmacia, Piscataway, NJ) and by exposure to Kodak X-OMAT AR film (Rochester, NY). To detect DNMT3b2 and 3b3 proteins in the human cell line panel (Fig. 3A), 60 μg of total protein from J82 and LD692 cells were required instead of 30 μg total protein from the remaining cell lines.

Nucleic Acid Isolation

RNA was collected from mouse ES cells and human cells under both untreated and treated conditions using the RNeasy Protect Mini kit (Qiagen, Inc., Valencia, CA) as described by the manufacturer. DNA was collected as described previously (56).

RT-PCR Analysis

Total RNA purified from cells (2.5 μg) or from tissue samples (Clontech Laboratories, Inc., Palo Alto, CA) was reverse transcribed using Moloney murine leukemia virus reverse transcriptase (Invitrogen, Carlsbad, CA) and random hexamers (Amersham-Pharmacia, Piscataway, NJ) in a total volume of 25 μl. RT-PCR amplification reactions of each of the expressed genes was performed with 100 ng cDNA, 10% DMSO, 100 μM deoxynucleotide triphosphates, Taq DNA polymerase (Sigma Chemical), and 1 μM primers. The RT-PCR primers for the three Dnmt3b splice sites are as follows: Dnmt3b 5′ end sense: 5′-GCG CAG CGA TCG GCG CCG GAG AT-3′ and antisense: 5′-CAT ACC CGG TGG CAC CCT CTT CTT CAG TCA-3′, Dnmt3b exons 10 and 11 sense: 5′-CTG GAG AGT CAC TGG AGG ACC AGC TGA AGC-3′ and antisense: 5′-CTC TCC TCA TCC TCC CCT CGG TCC TTC-3′, Dnmt3b catalytic sense: 5′-AAG CCC ATG CAA TGA TCT CTC TAA CG-3′ and antisense: 5′-CAC GTC CGT GTA GTG AGC AGG GAA GC-3′, H4F2 sense: 5′-GCC CTG GCG CTT GAG CGC GT-3′ and antisense: 5′-TCG GGT CGC GGC AAG GGA GGA-3′, human PCNA sense: 5′-CAA CTT GGA AT CCA GAA CAG GAG TAC AGC-3′ and antisense: 5′-GGG TAC ATC TGC AGA CATR ACT GAG TGT CA-3′, and human DNMT3b exons 10 and 11 sense: 5′-AGC CCA TGT TGG AGT GGG CCC ACG-3′ and antisense: 5′-CAT CCC CTC GGT CTT TGC CGT TGT TAT-3′. The RT-PCR conditions and primers to amplify the catalytic domain of human DNMT1, 3a, and 3b and glyceraldehyde-3-phosphate dehydrogenase were previously shown (24). Gels were hybridized to GeneScreen Plus membranes (Perkin-Elmer Corp., Boston, MA) and probed with ^{32}P-labeled oligomeric probes for each DNMT as previously described (24). The ratios of expression of DNMT3b3 to DNMT3b2 mRNA were determined by comparing the intensities of the bands corresponding to each DNMT3b isoform by phosphorimager analysis.

Southern Blot Analysis

Genomic DNA (5 μg) was digested with 10 units/μg *Hpa*II or *Msp*I, fractionated on a 1% agarose gel, and transferred to a nylon membrane (GeneScreen; Perkin Elmer Corp., Boston, MA) in 10× SSC. The blots were probed with ^{32}P-end-labeled oligomer probes to represent the consensus sequences for satellite 2 (5′-TCG AGT CCA TTC GAT GAT-3′) and satellite 3 (5′-TCC ACT CGG GTT GATT-3′) in Church buffer [500 mM $NaPO_4$ (pH 6.8), 1 mM EDTA (pH 8.0), and 7% SDS] at 42°C overnight, and the blots were washed twice in 2× SSC and 0.1% SDS and twice in 0.2× SSC and 0.5% SDS at room temperature. Bands were visualized by autoradiography.

Bisulfite-Specific PCR and Ms-SNuPE Reactions

Mouse ES and human T24 genomic DNA (4 μg) were bisulfite treated as previously described (39). The bisulfite-specific PCR and the qualitative Ms-SNuPE assays for the *p16* promoter and *p16* exon 2 sequences were performed as previously described (38). The bisulfite-specific PCR primers for the *p53* Alu are as follows: sense: 5′-TGG GTT TAA TTA TTG TAT AGT TGA A-3′ and antisense: 5′-CTC AAC TCA CTA CAA ACT CCA-3′ and the *D4Z4* bisulfite-specific PCR primers are as follows: sense: 5′-GGG TTG AGG GTT GGG TTT AT-3′ and antisense: 5′-AAC TTA CAC CCT TCC CTA CA-3′. The PCR conditions for the *p53* Alu were 95°C for 3 min followed by 40 cycles of denaturation at 95°C for 1 min, annealing at 52°C for 45 s, and extension at 72°C for 45 s. The *D4Z4* PCR was performed in the same manner, except that the annealing temperature was 58°C. A final 10-min extension at 72°C completed each PCR program. The Ms-SNuPE conditions for *p53* Alu and *D4Z4* were the same as those described previously (38). The Ms-SNuPE primers for the *p53* Alu are as follows: 5′-GTT AAG GGT TTT TTT TGT TTG GTT GGG-3′, 5′-TTT GGG AGG TTA AGG TAG G-3′, 5′-GTT TTT ATT GAA AAA TAT AAA AAA AAA TTA GT-3′, and 5′-GAA GGA GAA TGG TGT GAA TTT GGG-3′. The *D4Z4* Ms-SNuPE primers are as follows: 5′-TGA GGG TTG GGT TTA TAG T-3′, 5′-GTG GTT TAG GGA GTG GG-3′, 5′-TAT ATT TTT AGG TTT AGT TTT GTA A-3′, and 5′-GAA AGG TTG GTT ATG T-3′.

Acknowledgments

We thank Dr. En Li for providing the wild-type and knockout ES cells, Dr. Peter Laird for providing the *Dnmt1* knockout ES cells and for helpful discussions, Dr. Gerhard Coetzee and members of his laboratory for helpful discussions, and the members of the Jones laboratory for support and helpful discussions.

References

1. Bird, A. DA methylation patterns and epigenetic memory. Genes Dev., *16:* 6–21, 2002.

2. Jones, P. A. and Baylin, S. B. The fundamental role of epigenetic events in cancer. Nat. Rev. Genet., *3:* 415–428, 2002.

3. Bird, A. The essentials of DNA methylation. Cell, *70:* 5–8, 1992.

4. Pradhan, S., Bacolla, A., Wells, R. D., and Roberts, R. J. Recombinant human DNA (cytosine-5) methyltransferase. I. Expression, purification, and comparison of *de novo* and maintenance methylation. J. Biol. Chem., *274:* 33002–33010, 1999.

5. Pradhan, S., Talbot, D., Sha, M., Benner, J., Hornstra, L., Li, E., Jaenisch, R., and Roberts, R. J. Baculovirus-mediated expression and characterization of the full-length murine DNA methyltransferase. Nucleic Acids Res., *25:* 4666–4673, 1997.

6. Yoder, J. A., Soman, N. S., Verdine, G. L., and, Bestor, T. H. DNA (cytosine-5)-methyltransferases in mouse cells and tissues. Studies with a mechanism-based probe. J. Mol. Biol., *270:* 385–395, 1997.

7. Li, E., Bestor, T. H., and Jaenisch, R. Targeted mutation of the DNA methyltransferase gene results in embryonic lethality. Cell, *69:* 915–926, 1992.

8. Okano, M., Bell, D. W., Haber, D. A., and Li, E. DNA methyltransferases Dnmt3a and Dnmt3b are essential for *de novo* methylation and mammalian development. Cell, *99:* 247–257, 1999.

9. Stewart, C. L., Stuhlmann, H., Jahner, D., and Jaenisch, R. *de novo* methylation, expression, and infectivity of retroviral genomes introduced into embryonal carcinoma cells. Proc. Natl. Acad. Sci. USA, *79:* 4098–4102, 1982.

10. Okano, M., Xie, S., and Li, E. Cloning and characterization of a family of novel mammalian DNA (cytosine-5) methyltransferases. Nat. Genet., *19:* 219–220, 1998.

11. Gowher, H. and Jeltsch, A. Enzymatic properties of recombinant Dnmt3a DNA methyltransferase from mouse: the enzyme modifies DNA in a non-processive manner and also methylates non-CpA sites. J. Mol. Biol., *309:* 1201–1208, 2001.

12. Ramsahoye, B. H., Biniszkiewicz, D., Lyko, F., Clark, V., Bird, A., and Jaenisch, R. Non-CpG methylation is prevalent in embryonic stem cells and may be mediated by DNA methyltransferase 3a. Proc. Natl. Acad. Sci. USA, *97:* 5237–5242, 2000.

13. Fuks, F., Burgers, W. A., Godin, N., Kasai, M., and Kouzarides, T. Dnmt3a binds deacetylases and is recruited by a sequence-specific repressor to silence transcription. EMBO J., *20:* 2536–2544, 2001.

14. Bachman, K. E., Rountree, M. R., and Baylin, S. B. Dnmt3a and Dnmt3b are transcriptional repressors that exhibit unique localization properties to heterochromatin. J. Biol. Chem., *276:* 32282–32287, 2001.

15. Hansen, R. S., Wijmenga, C., Luo, P., Stanek, A. M., Canfield, T. K., Weemaes, C. M. R., and Gartler, S. M. The *DNMT3B* DNA methyltransferase gene is mutated in ICF immunodeficiency syndrome. Proc. Natl. Acad. Sci. USA, *96:* 14412–14417, 1999.

16. Xu, G-L., Bestor, T. H., Bourc'his, D., Hsieh, C., Tommerup, N., Bugge, M., Hulten, M., Qu, X., Russo, J. J., and Viegas-Pequignot, E. Chromosome instability and immunodeficiency syndrome caused by mutations in a DNA methyltransferase gene. Nature, *402:* 187–190, 1999.

17. Liang, G., Chan, M., Tomigahara, Y., Tsai, Y. C., Gonzales, F. A., Li, E., Laird, P. W., and Jones, P. A. Cooperativity between DNA methyltransferases in the maintenance methylation of repetitive elements. Mol. Cell. Biol., *22:* 480–491, 2002.

18. Rhee, I., Bachman, K. E., Park, B. H., Jair, K. W., Yen, R. W., Schuebel, K. E., Cui, H., Feinberg, A. P., Lengauer, C., Kinzler, K. W., Baylin, S. B., and Vogelstein, B. DNMT1 and DNMT3b cooperate to silence genes in human cancer cells. Nature, *416:* 552–556, 2002.

19. Kim, G. D., Ni, J., Kelesoglu, N., Roberts, R. J., and Pradhan, S. Co-operation and communication between the human maintenance and *de novo* DNA (cytosine-5) methyltransferases. EMBO J., *21:* 4183–4195, 2002.

20. Robertson, K. D. DNA methylation, methyltransferases and cancer. Oncogene, *20:* 3139–3155, 2001.

21. Cheng, X. Structure and function of DNA methyltransferases. Annu. Rev. Biophys. Biomol. Struct., *24:* 293–318, 1995.

22. Kumar, S., Cheng, X., Klimasauskas, S., Mi, S., Posfai, J., Roberts, R. J., and Wilson, G. G. The DNA (cytosine-5) methyltransferases. Nucleic Acids Res., *22:* 1–10, 1994.

23. Margot, J. B., Aguirre-Arteta, A. M., Di GIacco, B. V., Pradhan, S., Roberts, R. J., Cardoso, M. C., and Leonardt, H. Structure and function of the mouse DNA methyltransferase gene: Dnmt1 shows a tripartite structure. J. Mol. Biol., *297:* 293–300, 2000.

24. Robertson, K. D., Uzvolgy, E., Liang, G., Talmadge, C., Sumegi, J., Gonzales, F. A., and Jones, P. A. The human DNA methyltransferases (DNMTs) 1, 3a and 3b: coordinate mRNA expression in normal tissues and overexpression in tumors. Nucleic Acids Res., *27:* 2291–2298, 1999.

25. Xie, S., Wang, Z., Okano, M., Nogami, M., Li, Y., He, W-W., Okumura, K., and Li, E. Cloning, expression and chromosome locations of the human *DNMT3* gene family. Gene, *236:* 87–95, 1999.

26. Chen, T., Ueda, Y., Xie, S., and Li, E. A novel Dnmt3a isoform produced from an alternative promoter localizes to euchromatin and its expression correlates with active *de novo* methylation. J. Biol. Chem., *277:* 38746–38754, 2002.

27. Aoki, A., Suetake, I., Miyagawa, J., Fujio, T., Chijiwa, T., Sasaki, H., and Tajima, S. Enzymatic properties of *de novo*-type mouse DNA (cytosine-5) methyltransferases. Nucleic Acids Res., *29:* 3506–3512, 2001.

28. Chen, T., Ueda, Y., Dodge, J. E., Wang, Z., and Li, E. Establishment and maintenance of genomic methylation patterns in mouse embryonic stem cells by Dnmt3a and Dnmt3b. Mol. Cell. Biol., *23:* 5594–5605, 2003.

29. Soejima, K., Fang, W., and Rollins, B. J. DNA methyltransferase 3b contributes to oncogenic transformation induced by SV40T antigen and activated Ras. Oncogene, *22:* 4723–4733, 2003.

30. Saito, Y., Kanai, Y., Sakamoto, M., Saito, H., Ishii, H., and Hirohashi, S. Overexpression of a splice variant of DNA methyltransferase 3b, DNMT3b4, associated with DNA hypomethylation on pericentromeric satellite regions during human hepatocarcinogenesis. Proc. Natl. Acad. Sci. USA, *99:* 10060–10065, 2002.

31. Robert, M. F., Morin, S., Beaulieu, N., Gauthier, F., Chute, I. C., Barsalou, A., and MacLeod, A. R. DNMT1 is required to maintain CpG methylation and aberrant gene silencing in human cancer cells. Nat. Genet., *33:* 61–65, 2003.

32. Lei, H., Oh, S. P., Okano, M., Juttermann, R., Goss, K. A., Jaenisch, R., and Li, E. *de novo* cytosine methyltransferase activities in mouse embryonic stem cells. Development, *122:* 3195–3205, 1996.

33. Michalowsky, L. A. and Jones, P. A. Differential nuclear protein binding to 5-azacytosine-containing DNA as a potential mechanism for 5-aza-2′-deoxycytidine resistance. Mol. Cell. Biol., *7:* 3076–3083, 1987.

34. Santi, D. V., Garrett, C. E., and Barr, P. J. On the mechanism of inhibition of DNA-cytosine methyltransferases by cytosine analogs. Cell, *33:* 9–10, 1983.

35. Santi, D. V., Norment, A., and Garrett, C. E. Covalent bond formation between a DNA-cytosine methyltransferase and DNA containing 5-azacytosine. Proc. Natl. Acad. Sci. USA, *81:* 6993–6997, 1984.

36. Robertson, K. D., Keyomarsi, K., Gonzales, F. A., Velicescu, M., and Jones, P. A. Differential mRNA expression of human DNA methyltransferases (DNMTs) 1, 3a, and 3b during the G_0/G_1 to S phase transition in normal and tumor cells. Nucleic Acids Res., *28:* 2108–2113, 2000.

37. Kondo, T., Bobek, M. P., Kuick, R., Lamb, B., Xhu, X., Narayan, A., Bourc'his, D., Viegas-Pequignot, E., Ehrlich, M., and Hanash, S. M. Whole-genome methylation scan in ICF syndrome: hypomethylation of non-satellite DNA repeats D4Z4 and NBL2. Hum. Mol. Genet., *9:* 597–604, 2000.

38. Velicescu, M., Weisenberger, D. J., Gonzales, F. A., Nguyen, C. T., and Jones, P. A. Cell division is required for *de novo* methylation of CpG island in cancer cells. Cancer Res., *62:* 2378–2384, 2002.

39. Bender, C. M., Gonzalgo, M. L., Gonzales, F. A., Nguyen, C. T., Robertson, K. D., and Jones, P. A. Roles of cell division and gene transcription in the methylation of CpG islands. Mol. Cell. Biol., *19:* 6690–6698, 1999.

40. Nguyen, C. T., Gonzales, F. A., and Jones, P. A. Altered chromatin structure associated with methylation-induced gene silencing in cancer cells: correlation of accessibility, methylation, MeCP2 binding and acetylation. Nucleic Acids Res., *29:* 4598–4606, 2001.

41. Magewu, A. N. and Jones, P. A. Ubiquitous and tenacious methylation of the CpG site in codon 248 of the p53 gene may explain its frequent appearance as a mutational hotspot in human cancer. Mol. Cell. Biol., *14:* 4225–4232, 1994.

42. Qiu, C., Sawada, K., Zhang, X., and Cheng, X. The PWWP domain of mammalian DNA methyltransferase Dnmt3b defines a new family of DNA-binding folds. Nat. Struct. Biol., *9:* 217–224, 2002.

43. Chen, L., MacMillan, A. M., Chang, W., Ezaz-Nikpay, K., Lane, W. S., and Verdine, G. L. Direct identification of the active-site nucleophile in a DNA (cytosine-5)-methyltransferase. Biochemistry, *30:* 11018–11025, 1991.

44. Wyszynski, M. W., Gabbara, S., Kubareva, E. A., Romanova, E. A., Oretskaya, T. S., Gromova, E. S., Shabarova, Z. A., and Bhagwat, A. S. The cysteine conserved among DNA cytosine methylases is required for methyltransfer, but not for specific DNA binding. Nucleic Acids Res., *21:* 295–301, 1993.

45. Klimasauskas, S., Kumar, S., Roberts, R. J., and Cheng, X. *Hha*I methyltransferase flips its target base out of the DNA helix. Cell, *76:* 357–369, 1994.

46. Gabbara, S. and Bhagwat, A. S. The mechanism of inhibition of DNA (cytosine-5-)-methyltransferases by 5-azacytosine is likely to involve methyl transfer to the inhibitor. Biochem. J., *307:* 87–92, 1995.

47. Reinisch, K. W., Chen, L., Verdine, G. L., and Lipscomb, W. N. The crystal structure of *Hae*III methyltransferase covalently complexed to DNA: an extrahelical cytosine and rearranged base pairing. Cell, *82:* 143–153, 1995.

48. Hurd, P. J., Whitmarsh, A. J., Baldwin, G. S., Kelly, S. M., Waltho, J. P., Price, N. C., Connolly, B. A., and Hornby, D. P. Mechanism-based inhibition of C5-cytosine DNA methyltransferases by 2-H-pyrimidinone. J. Mol. Biol., *286:* 389–401, 1999.

49. Brank, A. S., Eritja, R., Guimil-Garcia, R., Marquez, V. E., and Christman, J. K. Inhibition of *Hha*I DNA (cytosine-C5) methyltransferase by oligodeoxyribonucleotides containing 5-aza-2′-deoxycytidine: examination of the intertwined roles of co-factor, target, transition state structure and enzyme conformation. J. Mol. Biol., *323:* 53–67, 2002.

50. Bourc'his, D., Xu, G-L., Lin, C. S., Bollman, B., and Bestor, T. H. Dnmt3L and the establishment of maternal genomic imprints. Science, *294:* 2536–2539, 2001.

51. Hata, K., Okano, M., Lei, H., and Li, E. Dnmt3L cooperates with the Dnmt3 family of *de novo* DNA methyltransferases to establish maternal imprints in mice. Development, *129:* 1983–1993, 2002.

52. Chedin, F., Lieber, M. L., and Hsieh, C-L. The DNA methyltransferase-like protein DNMT3L stimulates *de novo* methylation by Dnmt3a. Proc. Natl. Acad. Sci. USA, *99:* 16916–16921, 2002.

53. Myohanen, S. K., Baylin, S. B., and Herman, J. G. Hypermethylation can selectively silence individual p16INK4A alleles in neoplasia. Cancer Res., *58:* 591–593, 1998.

54. Markl, I. D. C. and Jones, P. A. Presence and location of TP53 mutation determines pattern of CDKN2A/ARF pathway inactivation in bladder cancer. Cancer Res., *58:* 5348–5353, 1998.

55. Weisenberger, D. J., Velicescu, M., Preciado-Lopez, M. A., Gonzales, F. A., Tsai, Y. C., Liang, G., and Jones, P. A. Identification and characterization of alternatively spliced variants of DNA methyltransferase 3a in mammalian cells. Gene, *298:* 91–99, 2002.

56. Gonzales-Zulueta M, Bender C. M., Yang, A. S., Nguyen, T. D., Beart, R. W., Van Tornout, J. M., and Jones, P. A. Methylation of the 5′ CpG island of the p16/CDKN2 tumor suppressor gene in normal and transformed human tissues correlates with gene silencing. Cancer Res., *55:* 4531–4535, 1995.